Surface modification of mesenchymal stromal cell-derived extracellular vesicles with peptides for targeted cancer therapy

Pedro Espírito Santo Prates Gonçalves*, Supervisors: Cláudia Lobato da Silva* and Nuno Bernardes*
* Instituto Superior Técnico, University of Lisbon, Portugal

Abstract
Conventional systemic cancer therapies are responsible to induce severe side effects. This limits the efficacy of the current therapeutic strategies, and this challenge needs to be addressed by novel approaches.
In the last decade, extracellular vesicles (EVs), phospholipid bilayer membrane structures released by all cells, have emerged as promising nano drug delivery systems (NDDS). These display amenability for loading with multiple anticancer therapeutics as well as for engineering aimed to improve their accumulation at the target tissues.
In order to develop an EV-based NDDS for targeted cancer therapy, in this work, EVs derived from mesenchymal stromal cells were isolated through a scalable and selective protocol comprising tangential flow filtration (TFF) and size exclusion chromatography (SEC). Here, the adjustment of upstream and downstream processing such as the cell confluence reached during expansion as well as the MWCO of amicons used for the EV ultrafiltration, were identified to be crucial parameters for increased batch yields.
Moreover, the EVs were decorated with a targeting moiety that includes p28, a peptide that displays a preferential penetration into cancer cells. The anchoring to EVs was achieved through the use of a novel fusion peptide combining p28 with CP05, which anchors itself in the surface of EVs by interacting with CD63. Incubation of breast cancer cells with EVs-p28 led to an increased cell uptake of EVs by 1,4-fold, showing their superiority as a NDDS.
Future work targeting the evaluation of the drug delivery efficiency of this system is important as it will allow a greater understanding of the potential application of the proposed NDDS.

Keywords: extracellular vesicles, mesenchymal stromal cells, p28, anti-cancer therapy, drug delivery systems, scalable production

1. Introduction

EVs are signalosomes that play a major role in cell-to-cell communication, being able to trigger phenotypic alterations in cells through surface interactions [1] and the delivery of their intraluminal cargo [2].
As more information became available about these entities, EVs began to emerge as promising systems to be used as NDDS since they overcome the limitations of synthetic nanocarriers. For instance, EVs are described to be more biocompatible and minimally toxic [3], as they naturally occur in the organism [9]. Additionally, EVs have an innate ability to cross biological barriers [4] and were proven to be more efficient in the delivery of RNAs to cells in comparison to a state-of-the-art synthetic nanocarrier [5].
However, to harness their potential as NDDS high quantities of EVs need to be isolated [1]. This can be problematic since the field is still lacking highly efficient isolation methodologies. Currently, methods still present certain limitations such as low yields [2]. And, the golden standard method, ultracentrifugation [3], is recognized for its detrimental impacts on the EV structure [4] and for limited scalability, which is also a major limitation considering that the treatment of patients will require large doses. Therefore, in this work, a gentle, scalable, and selective EV isolation methodology, comprised of TFF combined with SEC was employed to isolate EVs from large quantities of conditioned medium [4], [5].
Additionally to employ EVs as effective NDDS their surface modification with specific targeting moieties is crucial to allow them to accumulate in the desired tissues at clinically relevant numbers upon systemic administration [6], [7].
To this end, multiple methodologies can be employed. For example, genetic engineering, which is based on the expression of transgenes or chimeric proteins that are known to be enriched into EVs, was already employed in multiple studies however this strategy is highly dependent on the degree of enrichment of these proteins into EVs, which can be a limitation. And it is a time-consuming technique that is hard to establish in primary cells [8]. Alternatives to this method, that target EVs instead of the producer cells are also available, namely, click chemistry [9] and modifications based on electrostatic interactions. For instance, Gao X et al, were already successful in anchoring a muscle-targeting peptide to the EV surface, by fusing it with CP05, a peptide that anchors itself to the EV surface through the interactions that it establishes with CD63 [10]. Considering the success of this CP05-based strategy, this peptide will be employed in this work as well. In this case to anchor p28 to the EV surface.
p28 is a small peptide with 28 amino acids (2.8 KDa) which is the protein transduction domain of azurin [11] holding the same anticancer properties, pro-apoptotic, and preferential entrance in tumor cells observed in this bacterial protein [12], [13]. As such, EVs functionalized with p28 may be able to target solid tumors more effectively.
Moreover, parent cell selection is also a crucial step for the successful development of an NDDS. This selection can have an impact on the qualities of the isolated EVs, in terms of the biological activity, cargo, tissue homing abilities, immunogenicity as well as carcinogenicity. Moreover, the selected cell type must be evaluated in terms of its usability for large-scale production.
As MSC-EVs were already described to exert similar therapeutic effects as MSC in animal models and humans [14]. And, since MSC are immune evasive,

i.e., they do not trigger the immune system, MSC-EVs, because of their reduced transmembrane content, are also not expected to trigger the immune system, being considered safer than their parent cells This opens the possibility for the creation of off-the-shelf products for heterologous therapies based on MSC-EVs. Additionally, because clinical-grade MSC are already cultured for years in the context of cell therapy applications, complying with the good manufacturing practices (GMP), robust platforms are already described for their expansion which can also be taken advantage of for EV production. Considering such characteristics and other inherently related to EVs such as the fact that they are non-mutagenic and do not replicate, MSC-EVs represent a promising alternative to MSC-based cell therapies [15], but also for the delivery of therapeutic agents to diseased tissues.

In sum, herein, MSC(BM)-EVs were produced in conditions closely translatable to clinical settings, through the application of S/X-F conditions as well as through the utilization of a GMP-compatible EV isolation method comprised of TFF combined with SEC. These EVs were decorated with the CD63 anchoring peptide CP05-p28. And finally, the impact of this modification on EV uptake by breast cancer cells was investigated.

2. Materials and Methods

MSC(BM) isolation from human samples

The human MSC(BM) used in this study are part of the cell bank available at the Stem Cell Engineering Research Group (SCERG), iBB - Institute for Bioengineering and Biosciences. MSC(BM) were isolated following an adapted version of the cell isolation protocol described by Santos et al. using human platelet lysate (hPL) - supplemented medium instead of fetal bovine serum (FBS) [16]. Human tissue utilized to isolate cells was obtained under a collaboration agreement of iBB-IST and Instituto Português de Oncologia, Francisco Gentil, Lisboa. These human samples were collected from healthy donors after informed written consent according to the Directive 2004/23/EC of the European Parliament and of the Council of 31 March 2004 on setting standards of quality and safety for the donation, procurement, testing, and processing, preservation, storage and distribution of human tissues and cells (Portuguese Law 22/2007, June 29) with the approval of the Ethics Committee of the clinical institution. Human MSC(BM) were cryopreserved in cryovials (ABDOS) in culture medium containing 10% (v/v) DMSO (Sigma Aldrich), in a liquid/vapor-phase nitrogen container.

Cell thawing

Both MSC(BM) and the cell line MDA-MB-231 kindly provided by Dr. Pieter Vader (UMC Utrecht) were utilized for EV production. Cryovials containing cells were retrieved from the cryostorage to be thawed. MDA-MB-231 were cryopreserved in cryovials (ABDOS) in culture medium containing 10% (v/v) DMSO (Sigma Aldrich), in a liquid/vapor-phase nitrogen container. MSC(BM) were thawed at P2, P3, or P4. And MDA-MB-231 were thawed at P13 and P19. After depressurizing the cryovial inside the flow hood and partially thawing the material in a 37ºC water bath, 5 mL of warm supplemented medium was used to fully thaw the cells.

For MSC(BM) DMEM low glucose (1 g/L) medium was supplemented with 5% (v/v) of hPL UltraGRO™ PURE (AventaCell Biomedical) and 1% Antibiotic-Antimycotic (Thermo Fisher Scientific). For MDA-MB-231 DMEM high glucose (4,5 g/L) was supplemented with 10% FBS, qualified (Gibco) and 1% Antibiotic-Antimycotic (Thermo Fisher Scientific). Centrifugation (ThermoFisher Scientific, Heraus Multifuge X1R Centrifuge) at 1250 rpm was performed for 7 minutes. And afterward, the supernatant was discarded, and the pellet was resuspended in the same culture medium where cells were initially thawed. Cells were counted using the Trypan Blue (Gibco) exclusion method and, finally, MSC(BM) were inoculated in T-flasks at a seeding density of 3000 - 4000 cells/cm^2, whereas one vial containing 1 million cells of the cell line MDA-MB-231 was inoculated in a T-25 flask. Culture conditions were maintained at 37ºC, and with 5% CO_2 in a humidified atmosphere.

The culture medium was changed every 3 - 4 days until MSC(BM) reached a 70 - 80 % confluency (qualitatively assessed) and until MDA-MB-231 reached an 80 - 90 % confluency.

Cell passage and expansion

At 70 - 80% cell confluency Tryple™ Select (Gibco), a xeno-free detaching solution was applied to MSC(BM) for 7 minutes, at 37ºC. For MDA-MB-231 when a confluency of 80-90% was reached 0,05% (v/v) trypsin (Thermo Fisher Scientific) with 0,1 mM EDTA (Sigma Aldrich) was applied for 4 minutes at 37ºC. After thawing MSC(BM) were passaged at least once before final inoculation into T-flasks for EV production at a seeding density of 3000 cells/cm^2. MDA-MB-231 were maintained in culture from P13 to P37 and expanded when intended to be utilized for EV production. These cells were seeded at 15 000 cells/cm^2 - 39 000 cells/cm^2.

EV production

After final inoculation for EV production in T-175 flasks cells were cultured in the same conditions described before. When maximum cell confluency, 90 - 100% was achieved, MSC(BM) and MDA-MB-231 were washed with DMEM low glucose basal medium (i.e. only supplemented with 1% Antibiotic-Antimycotic) and DMEM high glucose, respectively. These basal culture mediums were used during the 48 hours conditioning period for MSC(BM) and the 24 hours conditioning period for MDA-MB-231. Additionally, for MDA-MB-231, OptiMEM™ I Reduced Serum Medium (Gibco) was also used as a conditioned medium

EV isolation from cell culture

After the conditioning period, the conditioned medium was collected and always maintained at 4ºC from this procedure onward. A 2000 x g, 15 minutes

centrifugation was performed, and the supernatant underwent a bottle top filtration with a 0.45 um filter (Thermo Fisher Scientific, Nalgene)**.** For tangential flow filtration (TFF) the Minimate EVO system (PALL) is equipped with the Minimate 100 KDa MWCO Omega Membrane (PALL). And afterward, the sample undergoes size exclusion chromatography (SEC) using a HiPrep 16/60 S-400 Sephacryl column (GE Healthcare) connected to an AKTA start system (GE Healthcare). The selected EV fractions eluted from SEC are filtered through a syringe 0.45 µm filter (Corning) and concentrated with Amicons^{R} Ultra - 15 Centrifugal Filter Unit with a molecular weight cut-off (MWCO) of 100 kDa (Merck MilliPore) or 30 kDa, or alternativelly Amicons^{R} Ultra - 4 Centrifugal Filter Unit with a molecular weight cut-off (MWCO) of 50 kDa (Merck MilliPore)

Protein Quantification

The Micro BCA™ Protein Assay Kit (Thermo Fisher Scientific) was used for the quantification of the total amount of protein in EV samples, following the guidelines for the microplate procedure provided by the manufacturer. EVs were lysed in 1x RIPA buffer (Thermo Fisher Scientific) for 10 minutes at room temperature before the quantification. Additionally, the equation obtained through the application of a linear fit to bovine serum albumin (BSA) standards was used to determine the protein concentration of each sample by measuring its absorbance. For each sample, two replicate measurements were performed. An equal final RIPA buffer concentration was used to prepare all standards and samples.

Nanoparticle tracking analysis (NTA)

NTA measurements were performed with a NanoSight LM10 instrument (Malvern) equipped with a sample chamber and a 405 nm laser. The NTA 3.1 software was utilized for capture and analysis. Before measurements, samples were diluted in PBS to obtain a final concentration in the range of 5 x10^{8} to 2 x10^{9} particles/mL. Each sample was recorded 10 times for 30 seconds using a scripted function for control and each new acquisition was achieved by pushing new sample to the detection chamber. The acquisition and post-acquisition settings were kept constant for all similar samples.

A detection threshold of 5 was set for all samples measured. The Camera level settings were set to 15 for measurements of the processed sample of EVs, the TFF filtrate, and concentrate as well as for the SEC-filtered fractions. Whereas, for the centrifuged and isolated conditioned medium and OptiMEM the camera level was set to 14.

Peptide synthesis

The CP05-p28 peptide was synthesized with a >95% purity by DG Peptides Co., Ltd. The peptides were dissolved in PBS to a final concentration of 4 mg/mL and stored at -20ºC until further use. The detailed peptide sequence and the molecular weight are shown in table 1.

Table 1 - Name, amino acid sequence, and molecular weight of the peptide used in the study. MW- Molecular Weight

Name	CP05-$(GGGGS)_2$-Myc-p28
Amino acid sequence	CRHSQMTVTSRL-GGGGSGGGGS-EQKLISEEDL-DDPKLYDKDLGSAMGDTVVGQMDAATSL
MW (g/mol)	6130.77

EV uptake studies

MSC(BM) derived EVs and MDA-MB-231 derived EVs were labelled with the fluorescent dye AlexaFluor 647 NHS Ester (Invitrogen™) This lyophilized dye was dissolved at a concentration of 10 mg/mL in dimethyl sulfoxide (DMSO) (Sigma Aldrich). The EVs were mixed with sodium bicarbonate (Sigma Aldrich) (pH 8.3m 100 mM final concentration) and 0,625% (v/v) of Alexa Fluor 647 NHS ester (Thermo Fisher Scientific) (10 mg/mL in DMSO), and the mixture was incubated for 1 hour at 37 ºC in a shaker incubator at 450 rpm, followed by a dilution in PBS and quenching of the reaction with 100 mM Tris-HCl (Invitrogen) for 20 minutes at room temperature, where agitation was performed every 5 minutes, for the whole 20 minutes in a final volume of 1 mL.

Through SEC, using an XK-16/20 column (GE Healthcare) packed with Sepharose CL-4B (Sigma Aldrich), the unbound dye was separated from labelled EVs. The fractions containing EVs were pooled and filtered through a syringe filter, 0.45 um, as well as concentrated using Amicons^{R} Ultra - 4 Centrifugal Filter Unit with an MWCO of 100 kDa (Merck MilliPore), 10 kDa or 3 kDa (Merck MilliPore) (Merck MilliPore).

Finally, the stained EVs are characterized through NTA, and the fluorescence of the sample is measured in a plate reader (Tecan, infinite M200 PRO).

Labeled EVs were incubated with the peptide with a ratio of 50 ug of peptide / 10^{10} particles, for 2 hours at room temperature (RT). After incubation, the unbound peptide was washed out using a 100 kDa or 50 kDa MWCO Amicon Ultra-15 centrifugal filter unit (Merck MilliPore). The centrifugation conditions were 3000 x g, at 4ºC for c.a. 3 minutes for 100 kDa Amicons and c.a. 5 minutes when using 50 kDa Amicons. Washing was performed 3 times with 4 mL of PBS filtering until a final volume of c.a. 100 uL.

MDA-MB-231 cells were seeded at 50,000 per well (156 250 cells/cm^2) in a flat bottom 96 well plate in DMEM high glucose supplemented with 10% FBS, qualified (Gibco) and 1% Antibiotic-Antimycotic (Thermo Fisher Scientific). After 24 hours, the labeled EVs decorated with the peptide were added to the cells, and the mixture was incubated for 4 hours in a humidified atmosphere at 37ºC, with 5%

CO_2. After the incubation period, cells were washed once with PBS, detached from the wells using 0,05% (v/v) trypsin (Thermo Fisher Scientific) with 1 mM EDTA (Sigma Aldrich), resuspended in culture medium, and transferred to FACS tubes. The tubes were centrifuged for 5 minutes at 350 x g, and the pellet was resuspended in FACS buffer (1 mM EDTA (Sigma Aldrich) with 2% of heat inactivated FBS, qualified (Gibco) in PBS). Lastly, cells were analysed on a Flow Cytometer (Becton Dickinson, FACSCalibur), and the results were further analysed with FlowJo software.

3. Results and Discussion

Cell confluence and heterogeneity in tissue flasks' surface distribution impact MSC-EV yield

The quantity of EVs produced in each of the batches performed in the context of this work (BM EVs SEC 3, BM EVs SEC 4, BM EVs SEC 5, BM EVs SEC 6, and BM EVs SEC 7) substantially oscillated, comprising values between 1.13 x 10^9 and 1.87 x 10^{10} MSC-EVs per T-175 culture flask (Figure 1A), or 3.06 x 10^{10} to 9.06 x 10^{10} EVs per batch. These differences can be attributed to changes in upstream or downstream processing conditions that can significantly modulate the quantity of EVs produced and isolated. Additionally, the degree of the scale-out also varied greatly, ranging from 25 to 48 T-flasks (Figure 1B).

The homogeneity in the cell distribution on the T-flask surface during expansion and the cell confluence at the beginning of the periods of cell conditioning fluctuated greatly among batches. Having a homogenous layer and highly confluent (90-100%) growing MSC during expansion is crucial for their survival during conditioning, where cells are cultured in a non-supplemented media and hence do not have at their disposal the growth factors that are vital to sustain cell survival. When heterogeneity is present, the cells located at the lower confluency zones significantly lose their viability during the period of conditioning, detaching from the flask. This was the case of batch BM EVs SEC 6, and it may account for the fact that this batch, among all others, presents a lower quantity of cells at the end of the conditioning period (Figure 2B). In such a situation it is challenging to achieve a homogenous cell layer. This is the case because cell proliferation at, a certain stage, results in over confluency in some areas, possibly leading to the detachment of these cells while, at the same time, in zones of decreased cell density cells reach normal confluency. Of note, larger surfaces, such as in T-175 culture flasks, are generally associated with higher heterogeneity that needs to be controlled so that it does not impact greatly the conditioning period.

A

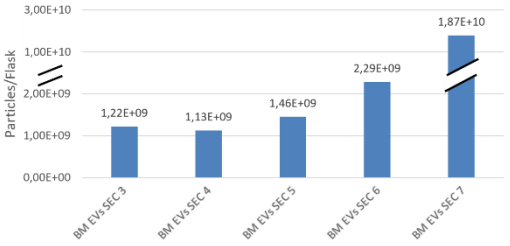

B

Assay No.	No. Cells/T-175	No. of T-175	Total No. Of EVs	MWCO of Amicons (kDa)
BM EVs SEC 3	3,28 x 10^6	25	3,06 x 10^{10}	100
BM EVs SEC 4	1,08 x 10^6	35	3,96 x 10^{10}	100
BM EVs SEC 5	1,73 x 10^6	40	5,83 x 10^{10}	50
BM EVs SEC 6	9,93 x 10^5	29	8,85 x 10^{10}	50
BM EVs SEC 7	2,75 x 10^6	48 (+1 x T-75)	9,06 x 10^{11}	30

C

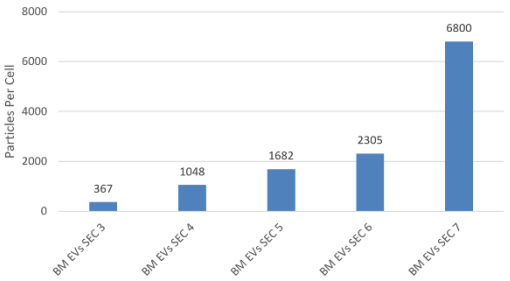

Figure 1 - **Production of MSC-EVs. A)** Number of particles isolated per T-175 culture flask. **B)** Comparison between batches considering the number of cells per T-175 flask at the end of the conditioning period, the size of each batch, i.e., the number of T-175 flasks (20 mL of cell culture medium each), the total number of particles isolated and the MWCO of the amicons ultra centrifugal units used in each batch. **C)** Quantity of particles produced by each cell, quantified at the final of the isolation protocol.

In batches BM EVs SEC 3, BM EVs SEC 4, and BM EVs SEC 5 even though moderate homogeneity was observed, the moderate confluence of cells (60% to 70%) led to losses in cell viability, during the conditioning period and as a result, fewer cells producing EVs leading to an overall decreased efficiency in terms of EV production. It is thus concluded that when confluences lower than 60% to 70% are present, it is not appropriate to switch to basal DMEM medium, because it will result in substantial cell death during the long 48 hours conditioning period. However, even though considerable losses of cell viability along with cell detachment were observed during these 48 hours, the cellular viability, of plastic-attached cells, was determined to be above 97% in all the assays, possibly because most of the dead cells detached from the plastic. This is an important parameter that should be captured at the end of conditioning periods since even a small percentage of cell death can release cell membranes to the cell-conditioned medium, which can outnumber the quantity of EVs released [149].

Only cells in T-flasks that reach high confluency (85 - 100%) were found to be robust enough to maintain viability and thrive under periods of conditioning, which was the case for BM EVs SEC 7. This may be associated with factors released by MSC to the extracellular space as well as the secretion of ECM, which may lead to higher gradients of concentration of these beneficial factors in high confluence areas that result in a boost in the cell robustness in such areas. However, these conclusions were reached only by observations at the phenotypic level. A more in-depth experience concerning cell stress, accessed for instance through the levels of lactate dehydrogenase (LDH) release or about cell metabolism when these are maintained in basal medium are required to obtain more quantitative data.

In the present work, the fine tuning of some procedures associated with the upstream processing was achieved, as can be observed by the increase of the EVs isolated per T-175 culture flask in the batch BM EVs SEC 7 in comparison to other MSC-EV batches, this was a substantial challenge as a limited number of EVs were obtained through several of the batches. As such the application of additional strategies to increase EV production may be necessary.

For example, the use of 3D dynamic upstream, e.g., hollow fiber, Vertical-Wheel^{TM} bioreactor, and stirred tank conditions may lead to obtaining severely higher yields of EVs [17]–[19]. Moreover, as bioreactors add options for dynamic monitoring of cell culture conditions, these may be beneficial for productions under GMP conditions. However, their implementation is not straightforward demanding extensive work and technical expertise to be handled, in comparison to 2D static approaches. Additionally, other modalities of MSC cultures, such as growth as suspended spheroids were already demonstrated to lead to increased EV production. The use of chemical or mechanical stimuli to induce EV production can also be applied. The stimulation conditions, among others, may comprise hypoxia, shear stress and the addition of anti-inflammatory drugs. However, those can also induce unpredictable changes in the characteristics of EVs which may affect their functional properties, and as such should be carefully analyzed. Moreover, the use of an MSC cell source that is more productive in terms of EV release than the BM can also be adopted. MSC from the Wharton's Jelly (WJ) were already reported to fit in that category. [18], [20]

Impact of the MWCO of amicons ultra centrifugal units in EV recovery

In this work, we tested different molecular weight cut-offs (MWCO) of the amicon ultra centrifugal units during the ultrafiltration (UF) applied to EVs after SEC separation. The objective was to evaluate how this factor influences the loss of EVs in the UF operation unit. In fact, it was noticed that a decrease in the MWCO leads to a slight increase in the EV yield (Figure 2A). This was evaluated through the SEC and amicon recoveries and assumes that the SEC recoveries remained constant among the assays.

A

Samples	TFF Recovery (%)	SEC and Amicon Recovery (%)	Total Recovery (%)	MWCO of Amicons (kDa)
BM EVs SEC 5	74	4	2,4	50
BM EVs SEC 6	88	4,7	4,2	50
BM EVs SEC 7	30	46	14	30

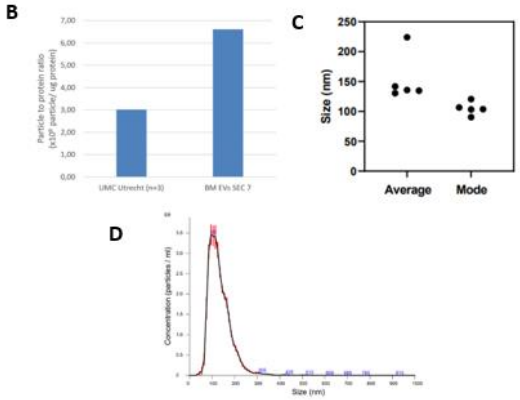

Figure 2- **Characteristics of MSC-EVs**. **A)** Comparison of the MSC-EV recovery through the various operation units of the EV isolation protocol. **B)** Comparison between the particle-to-protein ratio (PPR) of batch BM EVs SEC 7 and previous work [21] developed with a similar experimental setup (UMC-Utrecht (n=3)). **C)** EV average size and mode of size (n=5, technical replicates). **D)** Representative NTA size distribution curves of MSC-EVs, obtained from BM EVs SEC 7. PPR - particle to protein ratio. TFF- Tangential Flow Filtration. SEC – Size Exclusion Chromatography NTA - Nanoparticle Tracking Analysis.

It was already reported that the utilization of MWCO amicons of 10 kDa yielded significantly higher particle recoveries in comparison to 100 kDa MWCO amicons [221], [222], being in alignment with our findings.

Moreover, it is widely recognized that during these concentration steps many of the EVs are lost because of adhesion, aggregation as well as destruction [221] and additional strategies aimed at further improving EV recoveries may encompass the pre-treatment of the membranes of amicons ultra centrifugal units to decrease non-specific adsorption of the EVs, which leads to their loss. Detergents such as 5% Tween 80 were already shown to decrease the unspecific membrane binding of compounds [223], however, possible remnant detergent can pose challenges to the isolation of EVs, and possibly leads to alterations in EV structure, something that may be worth to investigate. Additionally, the problems of non-specific membrane binding render the UF process more time inefficient since it leads to a decreased filtrate flux.

In addition, similarly to the quantity of EVs isolated in each batch, the MSC-EV productivity also oscillated substantially, being comprised in between 367 and 6800 EVs released per cell (Figure 1C). This is possibly associated with batch variability in terms of cell homogeneity and viability, however, the MWCO of amicon ultra centrifugal units used for

SEC-isolated EVs UF also impacted the total number of EVs isolated from each batch.

EV characteristics

The average size of MSC-EVs did not change substantially through the assays, except for BM EVs SEC 4 where EVs present a higher mean (Figure 2C). This batch appears to be an outlier among the rest. Thus, excluding this batch, both the average size and mode of MSC-EVs are below 200 nm, which is in the interval of sizes characteristics of small EVs (up to 200 nm). However, the NTA size distribution curves of MSC-EVs obtained with NTA (Figure 2D) show populations of EVs with sizes above 200 nm, demonstrating that both small EVs, in much higher proportions, and larger EVs are isolated.

Regarding the characteristics of the isolated EV-based product, in batch BM EVs SEC 7 the particle-to-protein ratio (PPR), a parameter used to evaluate the purity of isolated EVs, was 6,60 x 10^9 particles / µg of protein which is more than twice the value that was obtained in preliminary work performed in UMC Utrecht (Figure 2B), showing that our optimizations in upstream and downstream processes can be leading to the co-isolation of a decreased quantity of protein content, increasing the purity of the sample. Overall, this parameter can indicate the reliability of the quantification of particle measure, as these can also detect protein aggregates.

MSC-EVs can be successfully labeled with Alexa Fluor™ 647 NHS Ester

After EV isolation the protocol of EV labeling is the following task when aiming to characterize possible improvements on cellular uptake. Separation of EVs from the unbounded dye after labeling is performed using SEC followed by concentration of EV-containing fractions by amicon-based UF.

Besides the amount of starting material and SEC-induced loss of EVs, the MWCO of amicons ultracentrifugal unit also influences the EV quantity to be recovered. In fact, envisaging to improve the yield of the UF, which is often substantially low, amicons of different MWCO were tested. A yield of 14% was determined when using an MWCO of 10 KDa and an 18% EV recovery was associated with ultrafiltration performed with 3 kDa amicon ultracentrifugal units (Figure 3A). This suggests an increase in EV recovery when lower MWCO are utilized. However. this conclusion is drawn from a limited number of experiments and as such should be confirmed in a more extensive evaluation. For instance, as this comparison is made between BM EVs SEC 6 and BM EVs SEC 7 the high discrepancy in the quantity of EVs yielded in both batches at the beginning of the process may also account for the variability observed in the ultrafiltration yields.

As shown in Figure 2B the higher the quantity of isolated EVs the higher the maximum absorbance intensity value displayed in the emission scans of the labeled EVs. For instance, in BM EVs SEC 7 higher intensities of fluorescence are observable in comparison with batches where lower amounts were isolated and were initially present at the beginning of labeling, e.g., BM EVs SEC 3, BM EVs SEC 4, and BM EVs SEC 5 and 6 (Pool).

A

Samples	Total Particle no. Before Staining	Total Particle no. After Staining	Yield (%)	Amicon MWCO (kDa)
BM EVs SEC 5 and 6 (Pool)	4,11 x 10^{10}	5,85x 10^9	14	10
BM EVs SEC 7	9,06 x 10^{11}	1,64 x 10^{11}	18	3

B

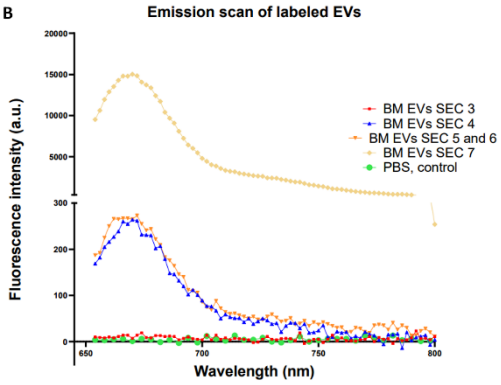

Figure 3 - EV staining with Alexa Fluor™ 647 NHS Ester. A) Comparison of MSC-EV yields in UF operation unit applied to labelled EVs. **B)** Comparison of the emission spectra of labelled MSC-EVs (excitation wavelength of 620 nm) of the different batches of MSC-EVs.

CP05-p28 anchorage to the surface of EVs

A fusion peptide conjugating CP05 and p28 was used to functionalize the surface of EVs. CP05 interacts with the tetraspanins CD63 present at the surface of EVs remaining anchored. This peptide was first used in a study developed by Gao, X et al. (2018) to functionalize EVs for the treatment of muscular dystrophia [22].

The fusion of p28 with the rest of the peptide was performed in its C terminal because the 18 amino acid residues localized in the N terminal are identified as being the minimal motif for the internalization of p28 [23]. As such, being the most important peptide terminal for cancer cell uptake it should remain free of constraints to naturally interact with other biological structures. Additionally, a linker, $(GGGGS)_2$ was inserted in the middle of the peptide to prevent steric hindrance in this targeting moiety, which allows p28 to be freely exposed. And a c-Myc tag was also placed in between p28 and CP05 (and not in any of the terminals) in order not to create impairments in the interaction of p28 with biological structures such as cells as well as of CP05 with CD63 present at the surface of EVs. In sum, the final design of the peptide employed for EV functionalization, which was developed in previous work in the context of this study [21], consisted of CP05 - $(GGGGS)_2$ - c-Myc - p28 (Figure 4A and 4B).

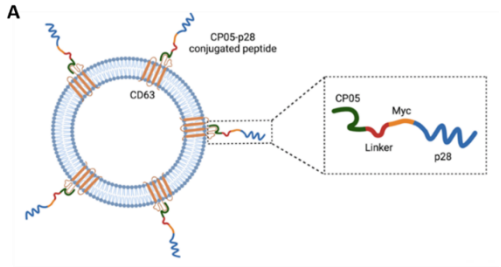

B

Nomenclature	Sequence
CP05	CRHSQMTVTSRL
p28	LSTAADMQGVVTDGMASGLDKDYLKPDD
Myc	EQKLISEEDL
Linker	$(GGGGS)_2$

Figure 4 - Design of the EV anchoring conjugated peptide CP05-p28. A) A diagram depicting the surface modification of EVs with CP05-p28. A peptide sequence (CP05) that anchors to CD63 on the EV surface, a $(GGGGS)_2$ linker, a Myc-tag reporter, and the p28 peptide (i.e., the 28 amino acid sequence Leu^{50}-Asp^{77} from the protein azurin) comprise the final peptide design. From de Almeida Fuzeta M. et al. (2021) [21]. **B)** Description of the sequences that are present in the design of CP05-p28. The sequences of the peptides are presented from the N-terminal (left) to the C-terminal (right).

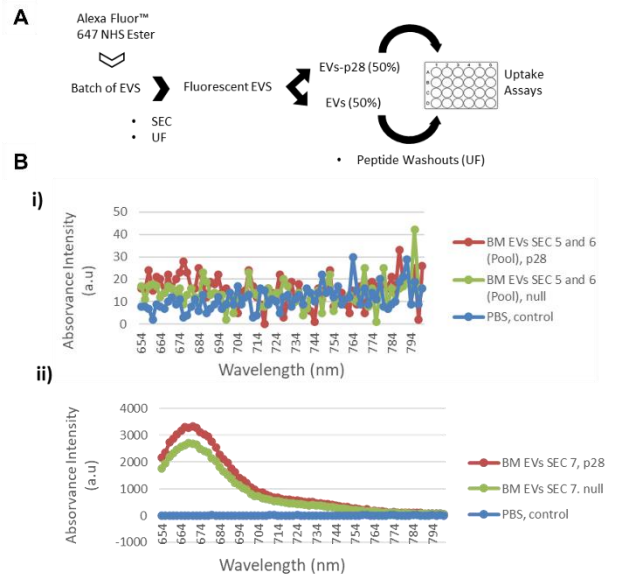

Figure 5 - Functionalization of EVs with CP05-p28 A) Scheme of the workflow employed for the labelling of each batch of EVs, as well as its functionalization and usage into assays of cell uptake. **B)** Emission spectrum (excitation wavelength of 620 nm) of functionalized and non-functionalized EVs. **i)** Batch where labelled functionalized and non-functionalized EVs did not display significant fluorescence in comparison with the negative control, PBS. **ii)** Batch where labelled, functionalized and non-functionalized, EVs displayed significant fluorescence in comparison with the negative control, PBS.

After the incubation of labeled EVs together with CP05-p28 the unbound peptide was separated from the functionalized EVs through UF in either 100 kDa or 50 kDa MWCO amicon ultra centrifugal units.

The number of washouts performed during this study was based on preliminary work [21] that showed that 3 washouts are sufficient for the unbound peptide to be eliminated (based on the detection of unbound peptide in amicon flowthrough by myc immunodetection)**.**

However, since the MWCO of the amicons used for this task was inferior to the 100 kDa previously used, an increased number of peptide washouts may be needed. This should be addressed in future work to guarantee that in uptake assays that follow there is no substantial contamination of EVs-p28 with unbound peptides, which could lead to a confounding effect, when both EVs-p28 and unbound p28 are administered together. For example, AFM demonstrated that azurin changed the membrane stiffness of lung cancer cells, increasing their permeability [24]. This can be the case for p28 in MDA-MB-231. The increase in the levels of unbound p28, because of their possible membrane modulation properties, can lead to increased membrane permeability and consequently to higher EV-p28 uptake, in comparison to pure EVs-p28. This does not allow a true assessment of how p28 EV functionalization impacts EV uptake on target cancer cells.

After anchorage of CP05 to the surface of MSC(BM)-EVs, and separation of the unbound peptide, the batches that previously emitted substantial fluorescence intensity after the staining assays, at this stage do not show any fluorescence intensity signal except for BM EVs SEC 7. The loss of EVs imposed by the yields associated with the peptide washouts performed by UF leads to losses in the amount of stained EVs, which ultimately causes a decrease in the fluorescence intensity detected. Only with a high enough quantity of starting material, in the order of magnitude of 10^{10} to 10^{11} EVs, such as in BM EVs SEC 7**,** it was possible to recover enough quantities of EVs that displayed a substantial fluorescence intensity in comparison to negative controls of PBS, figure 5B.

Of note, is that the functionalization of EVs with CP05-p28 is only performed with half of the labeled EVs per batch. The other half of the EVs, the null condition, will be used as a non-functionalized control in the assays that follow (Figure 5A). However, both samples are subjected to the same procedure, except that the incubation of EVs in the null condition is made with PBS and not with CP05-p28.

EV uptake by breast cancer cells increases upon CP05-p28 anchorage to the surface of MSC-EVs

For batch BM EVs SEC 7, where fluorescence was detected after CP05-p28 functionalization, we performed uptake assays with all the experimental conditions. The treatment of breast cancer cells with EVs-p28 led to a 1,4-fold increase in the MFI of cells in comparison to non-functionalized EVs (EVs) (Figure 6A, iii), suggesting that the functionalization of EVs with p28 (EVs-p28) leads to an increase in their uptake by MDA-MB-231. The preliminary work done in the context of this study [21] demonstrated

that breast cancer cells treated with EVs-p28 show an increase in uptake of 2,4-fold in comparison to non-functionalized EVs. Thus, EV functionalization through CP05-p28 anchorage may lead to values comprised between a 1,4 - 2,4-fold increase in the uptake of EVs in triple-negative breast cancer cells.
The impact of the dosage of EVs-p28 on their uptake by breast cancer cells was also evaluated. With this aim, two conditions were tested, EVs-p28, high and low, where the low dosage consisted approximately in half of the higher dose, 1,40 x 10^9 and 2,95 x 10^9 total number of fluorescently-labeled EVs-p28, respectively. The oscillation of the MFI induced by the different dosages administered to cells was proportional to the amount of EVs administered, figure 6B. In the low dose regime (n=1) the MFI was approximately half of what was observed in the high dose (n=2, technical replicate).
To further evaluate the impact of p28 on EV cell uptake future studies making use of CP05-p28Scrbl, where a scrambled sequence of p28 is present instead of the original one, should be performed. The use of these functionalized EVs in uptake assays can confirm the impact p28 sequence and its consequential 3D structure in the increased uptake that is observed when EVs-p28 were administered to breast cancer cells. If p28 is responsible for the increased EV-p28 uptake by cancer cells, CP05-p28 functionalized EVs will display increased uptakes in comparison to EVs modified with CP05-p28Scrbl.
In this work, the functionalization of EVs was achieved through a direct approach, allowing for a fast establishment of EVs-p28, to achieve the proof of concept that p28 drives a preferential penetration of EVs into cancer cells when used as a targeting moiety. However, it will be interesting to investigate how the quantity of CP05-p28 anchored to EVs affects their increased targeting capabilities towards cancer cells. If there is a significant dependency, it can be hypothesized that alterations on the levels of CD63 present in the surface of EVs can shape their ability to be endowed with increased targeting abilities through CP05-p28 anchorage. And since it is the case that the abundance of CD63 can vary on EVs secreted by different cell types, trying to implement this mechanism of functionalization in EVs derived from other cells may also lead to increased targeting abilities.
Additionally, the decoration of EVs with CP05-p28 does not occur through a covalent interaction. As such it can lead to a detrimental degree of instability at the level of the anchorage of this targeting moiety, which can be detrimental for the use of EVs-p28 as a NDDS since it can cause the detachment of CP05-p28 from the surface of EVs. Therefore, in future studies, it may be valuable to investigate other approaches for the functionalization of EVs, that allow for stabler anchoring. In fact, it is also possible to achieve a direct surface modification of EVs established through covalent interactions through click chemistry, which was already used successfully in several studies [9], [25] for the enhancement of EV-targeting abilities. And, recently, Pham TC *et al.* described a system of direct EV engineering that through protein ligases permitted a covalent binding to be established between EGFR-targeting peptides or anti-EGFR targeting nanobodies and EVs which facilitated their accumulation in EGFR-positive cancers *in vivo* [26]. And this method is suitable for targeting other receptors such as HER2.

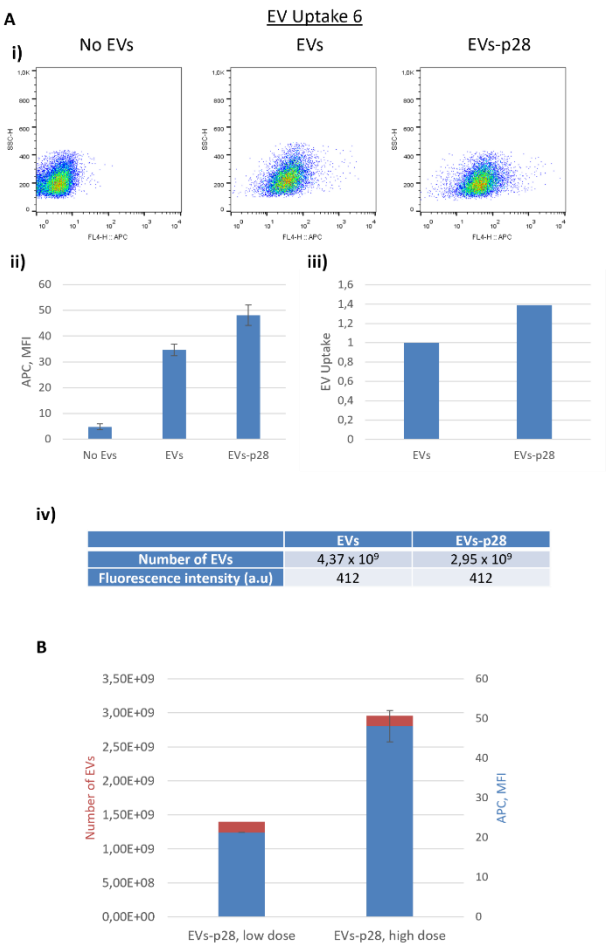

Figure 6 - Decoration of MSC-EVs with CP05-p28 increased the uptake of EVs by triple negative and metastatic breast cancer cells, MDA-MB-231. **A) i)** Flow Cytometry analysis of the EV uptake by breast cancer cells, where EVs functionalized with CP05-p28 display an increase in the EV uptake into cells, the x-axis represents the EV florescence height and the y-axis represents the side scatter (n= 2 technical replicates). **ii)** Median fluorescence intensity (MFI) of flow cytometry (n= 2 technical replicates). **iii)** Relative EV uptake based on the MFI values. **iv)** Comparison between the quantity of EVs administered to breast cancer cells and their absorbance intensity, in the different conditions tested, i.e. non-functionalized EVs (EVs) and CP05-p28 conjugation peptide-functionalized EVs (EVs-p28). **B)** Comparison between the median fluorescence intensity (MFI) of flow cytometry when EVs-p28 are administered in different dosages to breast cancer cells (n=1, EVs-p28, low dose, and n=2 technical replicates, EVs-p28, high dose). MFI - median intensity fluorescence.

In terms of indirect approaches to the engineering of EVs, genetic engineering, which is based on the expression of transgenes or chimeric proteins that are known to be enriched into EVs, can be used for EV surface modification and drug loading. However, for surface engineering, this strategy is highly dependent on the degree of enrichment of these

proteins into EVs, which can be a limitation. And it is a time-consuming technique that is hard to establish in primary cells [27]. However, once the cell engineering is successfully achieved it is substantially less laborious than direct interventions not requiring intense EV processing and separation from other substances (e.g., unbound targeting moieties aimed to be anchored on the surface of EVs) which not only severely impact the EV yield but can also affect EV biophysical properties and functional characteristics. In sum, both approaches (direct and indirect EV reconfigurations) may be advantageous depending on the final desired EV characteristics and their downstream application.

The optimization and reproducibility of EV surface engineering approaches aimed at improving EVs targeting abilities are crucially important for their clinical application since the systemic administration of naive EVs, i.e., non-functionalized EVs leads, mostly to their accumulation in organs such as the liver, spleen, and lungs [7], [28]–[30]. Consequently, EV decoration with targeting moieties may be an essential part of their clinical utilization.

When EV functionalization aims to achieve an increased target of cancer cells, several types of molecules were already utilized, such as peptides and aptamers. These moieties are generally targeted to specific overexpressed receptors on the surface of cancer cells, such as the HER2 [26] and EGFR [29], [31].

Regarding p28, it is described to preferentially penetrate a variety of solid tumors. Thus, although this study was performed in breast cancer cells, it has the potential to be extended to different types of solid tumors. Studies testing this hypothesis can ultimately yield insights concerning an increased penetration efficiency of the NDDS towards specific tumors, showing the most suitable cancers to be treated with this system. Moreover, a polymeric nanocarrier was already decorated with p28 to increase its targeting ability toward A549 lung cancer cells. In fact, this NDDS that was loaded with Gefitinib reduced the primary and metastatic tumor burden in tumor-bearing mice [32]. Evidencing the ability of p28 to be employed as a targeting moiety of nanoparticles aimed at the treatment of cancer. Moreover, the functionalization of these polymeric nanoparticles, lead to an increase of approximately 1,5-fold in lung cancer cell uptake in comparison to non-functionalized particles. This is a similar value to what was obtained in the present study, (1,4-fold to 2,4-fold increase) and it could demonstrate that p28 functionalization may lead to similar increases in nanoparticle penetration, despite the type of particle that is utilized. Overall, because of EVs' advantages over synthetic nanocarriers, such as increased biocompatibility, the use of EVs may be a safer choice when considering both options. Nonetheless, all things considered, two independent research studies investigating different types of nanoparticles and studying different types of solid tumors found similar results. When used as a targeting moiety, p28 was able to increase nanoparticle uptake by cancer cells.

Additionally, uptake assays comparing the uptake of EVs-p28 into normal cells and their cancerous counterparts will allow for the study of the specificity of the system.

In sum, in our work, it is the first time, to the best of our knowledge, that p28 is employed as a targeting moiety of EVs. And through this functionalization of EVs, which were produced in conditions that can be readily translated to clinical settings using S/X-F conditions and employing the GMP-compatible scalable and selective isolation method comprised of TFF-SEC, it was shown that MSC(BM)-EVs-p28 are preferentially uptake by breast cancer cells in comparison to non-functionalized MSC(BM)-EVs. Overall, the use of EVs-p28 as a new NDDS demonstrated to be a promising therapeutic approach that displays improved targeting of solid tumors.

4. Conclusions and Future Perspectives

In the present work, with the aim of developing an EV-based NDDS for targeted cancer therapy, p28, a peptide from the bacterial protein azurin that preferentially penetrates multiple solid tumors, was anchored to the surface of EVs, to test the hypothesis that it would improve EV uptake by cancer cells. For this purpose, a novel conjugation peptide, CP05-p28, previously developed by our group was utilized for this functionalization [21].

Moreover, we employed S/X-F cell culture conditions to produce human MSC(BM)-EVs and isolated the EVs from the cell culture-conditioned medium through TFF combined with SEC, a GMP-compatible scalable and selective isolation procedure. Since this method was not yet fully implemented in our lab facilities, it was established during the time of the present work. Of note is that these production conditions render this bioprocessing pipeline closely translatable to clinical practice. Additionally, this EV isolation method was established not only for primary cells but also for the immortalized cell line, MDA-MB-231, a breast cancer cell line.

The major finding of the study was that MSC(BM)-EVs-p28 uptake by triple-negative breast cancer cells was increased by 40% in comparison to its non-functionalized counterparts. Based on preliminary studies [188], it can be concluded that the increase of MSC(BM)-EVs-p28 uptake by breast cancer cells should range between 40% and 140% suggesting that this novel system could be valuable in efficiently delivering anticancer agents that have associated off-target effects.

The functionalization of MDA-MB-231-derived EVs was also tested, however, the low yields, similarly to what was observed in multiple batches of MSC-EVs, ultimately prevented conclusive findings, when exploring the functionalization of these EVs.

In fact, low EV yields were a major challenge faced in this study as well as a limitation because restricted conclusive technical replicates were performed in assays of EV-p28 uptake by cancer cells. This could have rendered the findings of the study substantially more robust.

And although EV yields were significantly increased in the last MSC-EV production, BM EVs SEC 7, mainly caused by the fine-tuning of cell culture conditions such as the achievement of high cell densities before conditioning, that led to higher amounts of EVs being produced and the use of MWCO amicons inferior to 100 kDa, that were advantageous for EV recovery, the implementation of a more efficient upstream processing could render EV production substantially more efficient and cost-effective.

Improvements in the process could rely on changing the expansion platform to multilayer T-flasks or 3D dynamic platforms, e.g., hollow-fiber, stirred tank, and the Vertical-Wheel^{TM} bioreactor, which are described to increase EV yields by several fold [17]–[19]. Chemical or mechanical cell stimuli can also cause cells to produce more EVs [33]–[35], and, additionally, the impact of different production media can be studied to this end. In fact, we evaluated the effect of using OptiMEM (i.e., an optimized formulation of Eagle's Minimal Essential Medium (MEM)) as an EV production medium and determined that although it can lead to an increase in EV production and cell robustness during periods of conditioning it leads to the contamination of the cell-derived EVs. Nonetheless, other promising options are available as well. For instance, RoosterBio^{R} offers the EV production medium RoosterCollect^{TM}-EV, which was already shown to increase EV production by cells, without substantial contamination [36], [37]. This could therefore be also tested using our experimental setup.

Overall, such strategies can likely lead not only to changes in the EV number but also in EV's biophysical and functional characteristics and investigation concerning this subject should follow such implementations. It should be noted as well that the conditions used in the upstream processing should be GMP compatible to operate in conditions that are more meaningful to clinical settings. Additionally, the MSC cell sources that are more productive such as the WJ can be adopted [20].

Moreover, in addition to the optimization of the upstream processing conditions, several challenges still must be overcome in the field of EVs to harness their full potential as therapeutic options. For instance, drug loading techniques available are still considered to have low efficiencies. And certain strategies such as genetic engineering, employed both for cargo loading and EV functionalization are difficult to implement especially in primary cells [38]. Importantly drug loading techniques as well as strategies aimed at EV surface modification should seek to be as efficient and reproducible as possible while maintaining EV integrity.

In addition, the selection of an appropriate cell source is also important. It should especially consider the downstream application of the EVs since their characteristics, such as the intraluminal molecules carried, are intrinsically related to the parent cell phenotype [2]. Moreover, additional variables such as cell availability, expandability, and EV productivity are also important to consider when choosing a parent cell source.

Concerning EV isolation, methods should be reproducible and efficient, as well as GMP-compatible and scalable. The balance between yield and purity should also be considered, and future EV-focused research will possibly solve this compromise. Interestingly, there is an increase in alternatives to the gold standard EV isolation technique, ultracentrifugation, [39] and this trend may continue to overcome ultracentrifugation's limitations. It is worth noting that filtration techniques, e.g. TFF and ultrafiltration, and SEC are a growing trend in the field [40].

Other challenges are that the EV characterization criteria as well as potency assays must be standardized to allow the comparison of findings throughout multiple laboratories. This will ultimately validate findings and thus prompt the clinical translation of EVs.

Additionally, more research will be needed to definitively determine ideal EV storage conditions, which could allow for their adoption as off-the-shelf products. Excipients such as trehalose and Tween 20 were already investigated and yielded promising results, in terms of EV recovery and cryodamage prevention [41] [42].

Furthermore, a greater understanding of EV biology, such as the processes governing endosomal escape following EV internalization and the attribution of specific traits to EV subpopulations can lead to the development of more effective EV-based therapeutic options.

In conclusion, the EV field is still in its infancy, and despite the significant obstacles that remain, there is now a vast research output that highlights their outstanding features and therapeutic qualities, when compared to synthetic nanocarriers and cell therapies, which will hopefully be leveraged for the effective treatment of several pathological conditions in the future.

5. Bibliography

[1] D. Gupta, A. M. Zickler, and S. el Andaloussi, 'Dosing extracellular vesicles', *Adv Drug Deliv Rev*, vol. 178, p. 113961, Nov. 2021, doi: 10.1016/J.ADDR.2021.113961.

[2] C. Paganini, U. Capasso Palmiero, G. Pocsfalvi, N. Touzet, A. Bongiovanni, and P. Arosio, 'Scalable Production and Isolation of Extracellular Vesicles: Available Sources and Lessons from Current Industrial Bioprocesses', *Biotechnol J*, vol. 14, no. 10, p. 1800528, Oct. 2019, doi: 10.1002/BIOT.201800528.

[3] F. Royo, C. Théry, J. M. Falcón-Pérez, R. Nieuwland, and K. W. Witwer, 'Methods for Separation and Characterization of Extracellular Vesicles: Results of a Worldwide Survey Performed by the ISEV Rigor and Standardization Subcommittee', *Cells*, vol. 9, no. 9, Aug. 2020, doi: 10.3390/CELLS9091955.

[4] F. Zhang *et al.*, 'Application of engineered extracellular vesicles for targeted tumor therapy', *J Biomed Sci*, vol. 29, no. 1, Dec. 2022, doi: 10.1186/S12929-022-00798-Y.

[5] S. Busatto *et al.*, 'Tangential Flow Filtration for Highly Efficient Concentration of Extracellular Vesicles from Large Volumes of Fluid', *Cells*, vol. 7, no. 12, Jan. 2018, doi: 10.3390/CELLS7120273.

[6] T. Smyth, M. Kullberg, N. Malik, P. Smith-Jones, M. W. Graner, and T. J. Anchordoquy, 'Biodistribution and delivery efficiency of unmodified tumor-derived exosomes', *Journal of Controlled Release*, vol. 199, pp. 145–155, Feb. 2015, doi: 10.1016/J.JCONREL.2014.12.013.

[7] M. Kang, V. Jordan, C. Blenkiron, and L. W. Chamley, 'Biodistribution of extracellular vesicles following administration into animals: A systematic review', *J Extracell Vesicles*, vol. 10, no. 8, Jun. 2021, doi: 10.1002/JEV2.12085.

[8] S. A. A. Kooijmans, R. M. Schiffelers, N. Zarovni, and R. Vago, 'Modulation of tissue tropism and biological activity of exosomes and other extracellular vesicles: New nanotools for cancer treatment', *Pharmacol Res*, vol. 111, pp. 487–500, Sep. 2016, doi: 10.1016/J.PHRS.2016.07.006.

[9] T. Smyth *et al.*, 'Surface functionalization of exosomes using click chemistry', *Bioconjug Chem*, vol. 25, no. 10, pp. 1777–1784, Oct. 2014, doi: 10.1021/BC500291R/SUPPL_FILE/BC500291R_SI_001.PDF.

[10] X. Gao *et al.*, 'Anchor peptide captures, targets, and loads exosomes of diverse origins for diagnostics and therapy', *Sci Transl Med*, vol. 10, no. 444, Jun. 2018, doi: 10.1126/SCITRANSLMED.AAT0195.

[11] T. Yamada, A. M. Fialho, V. Punj, L. Bratescu, T. K. das Gupta, and A. M. Chakrabarty, 'Internalization of bacterial redox protein azurin in mammalian cells: entry domain and specificity', *Cell Microbiol*, vol. 7, no. 10, pp. 1418–1431, Oct. 2005, doi: 10.1111/J.1462-5822.2005.00567.X.

[12] M. A. Warso *et al.*, 'A first-in-class, first-in-human, phase I trial of p28, a non-HDM2-mediated peptide inhibitor of p53 ubiquitination in patients with advanced solid tumours', *Br J Cancer*, vol. 108, no. 5, pp. 1061–1070, Mar. 2013, doi: 10.1038/BJC.2013.74.

[13] R. R. Lulla *et al.*, 'Phase I trial of p28 (NSC745104), a non-HDM2-mediated peptide inhibitor of p53 ubiquitination in pediatric patients with recurrent or progressive central nervous system tumors: A Pediatric Brain Tumor Consortium Study', *Neuro Oncol*, vol. 18, no. 9, pp. 1319–1325, Sep. 2016, doi: 10.1093/NEUONC/NOW047.

[14] J. Galipeau and L. Sensébé, 'Mesenchymal Stromal Cells: Clinical Challenges and Therapeutic Opportunities', *Cell Stem Cell*, vol. 22, no. 6, pp. 824–833, Jun. 2018, doi: 10.1016/J.STEM.2018.05.004.

[15] S. el Andaloussi, I. Mäger, X. O. Breakefield, and M. J. A. Wood, 'Extracellular vesicles: biology and emerging therapeutic opportunities', *Nature Reviews Drug Discovery 2013 12:5*, vol. 12, no. 5, pp. 347–357, Apr. 2013, doi: 10.1038/nrd3978.

[16] F. dos Santos, P. Z. Andrade, J. S. Boura, M. M. Abecasis, C. L. da Silva, and J. M. S. Cabral, 'Ex vivo expansion of human mesenchymal stem cells: a more effective cell proliferation kinetics and metabolism under hypoxia', *J Cell Physiol*, vol. 223, no. 1, pp. 27–35, Apr. 2010, doi: 10.1002/JCP.21987.

[17] A. Rutt, K. Bio, and J. J. Cadwell, 'Clinical Scale Production and Wound Healing Activity of Human Adipose Derived Mesenchymal Stem Cell Extracellular Vesicles from a Hollow Fiber Bioreactor'.

[18] R. A. Haraszti *et al.*, 'Exosomes Produced from 3D Cultures of MSCs by Tangential Flow Filtration Show Higher Yield and Improved Activity', *Mol Ther*, vol. 26, no. 12, pp. 2838–2847, Dec. 2018, doi: 10.1016/J.YMTHE.2018.09.015.

[19] M. de Almeida Fuzeta *et al.*, 'Scalable Production of Human Mesenchymal Stromal Cell-Derived Extracellular Vesicles Under Serum-/Xeno-Free Conditions in a Microcarrier-Based Bioreactor Culture System', *Front Cell Dev Biol*, vol. 8, p. 553444, 2020, doi: 10.3389/fcell.2020.553444.

[20] M. de Almeida Fuzeta *et al.*, 'Scalable Production of Human Mesenchymal Stromal Cell-Derived Extracellular Vesicles Under Serum-/Xeno-Free Conditions in a Microcarrier-Based Bioreactor Culture System', *Front Cell Dev Biol*, vol. 8, Nov. 2020, doi: 10.3389/FCELL.2020.553444.

[21] M. de Almeida Fuzeta, 'Scalable Production of Extracellular Vesicles Derived from Mesenchymal Stromal Cells for Cancer-Targeted Drug Delivery', 2021.

[22] X. Gao *et al.*, 'Anchor peptide captures, targets, and loads exosomes of diverse origins for diagnostics and therapy', *Sci Transl Med*, vol. 10, no. 444, p. eaat0195, 2018, doi: 10.1126/scitranslmed.aat0195.

[23] B. N. Taylor *et al.*, 'Noncationic peptides obtained from azurin preferentially enter cancer cells', *Cancer Res*, vol. 69, no. 2, pp. 537–546, Jan. 2009, doi: 10.1158/0008-5472.CAN-08-2932.

[24] N. Bernardes, S. Abreu, F. A. Carvalho, F. Fernandes, N. C. Santos, and A. M. Fialho, 'Modulation of membrane properties of lung cancer cells by azurin enhances the sensitivity to EGFR-targeted therapy and decreased β1 integrin-mediated adhesion', *Cell Cycle*, vol. 15, no. 11, p. 1415, Jun. 2016, doi: 10.1080/15384101.2016.1172147.

[25] W. Nan, C. Zhang, H. Wang, H. Chen, and S. Ji, 'Direct Modification of Extracellular Vesicles and Its Applications for Cancer Therapy: A Mini-Review', *Front Chem*, vol. 10, p. 538, May 2022, doi: 10.3389/FCHEM.2022.910341/BIBTEX.

[26] T. C. Pham *et al.*, 'Covalent conjugation of extracellular vesicles with peptides and nanobodies for targeted therapeutic delivery', *J Extracell Vesicles*, vol. 10, no. 4, p. e12057, Feb. 2021, doi: 10.1002/JEV2.12057.

[27] S. A. A. Kooijmans, R. M. Schiffelers, N. Zarovni, and R. Vago, 'Modulation of tissue tropism and biological activity of exosomes and other extracellular vesicles: New nanotools for cancer treatment', *Pharmacol Res*, vol. 111, pp. 487–500, Sep. 2016, doi: 10.1016/J.PHRS.2016.07.006.

[28] T. Smyth, M. Kullberg, N. Malik, P. Smith-Jones, M. W. Graner, and T. J. Anchordoquy, 'Biodistribution and delivery efficiency of unmodified tumor-derived exosomes', *Journal of Controlled Release*, vol. 199, pp. 145–155, Feb. 2015, doi: 10.1016/J.JCONREL.2014.12.013.

[29] S. A. A. Kooijmans *et al.*, 'PEGylated and targeted extracellular vesicles display enhanced cell specificity and circulation time', *Journal of Controlled Release*, vol. 224, pp. 77–85, Feb. 2016, doi: 10.1016/J.JCONREL.2016.01.009.

[30] C. P. Lai *et al.*, 'Dynamic biodistribution of extracellular vesicles in vivo using a multimodal imaging reporter', *ACS Nano*, vol. 8, no. 1, pp. 483–494, Jan. 2014, doi: 10.1021/NN404945R/SUPPL_FILE/NN404945R_SI_001.PDF.

[31] S. A. A. Kooijmans, J. J. J. M. Gitz-Francois, R. M. Schiffelers, and P. Vader, 'Recombinant phosphatidylserine-binding nanobodies for targeting of extracellular vesicles to tumor cells: a plug-and-play approach', *Nanoscale*, vol. 10, no. 5, pp. 2413–2426, Feb. 2018, doi: 10.1039/C7NR06966A.

[32] A. R. Garizo *et al.*, 'p28-functionalized PLGA nanoparticles loaded with gefitinib reduce tumor burden and metastases formation on lung cancer', *J Control Release*, vol. 337, pp. 329–342, Sep. 2021, doi: 10.1016/J.JCONREL.2021.07.035.

[33] J. Zhu *et al.*, 'Myocardial reparative functions of exosomes from mesenchymal stem cells are enhanced by hypoxia treatment of the cells via transferring microRNA-210 in an nSMase2-dependent way', *Artif Cells Nanomed Biotechnol*, vol. 46, no. 8, pp. 1659–1670, Nov. 2018, doi: 10.1080/21691401.2017.1388249.

[34] D. B. Patel, C. R. Luthers, M. J. Lerman, J. P. Fisher, and S. M. Jay, 'Enhanced extracellular vesicle production and ethanol-mediated vascularization bioactivity via a 3D-printed scaffold-perfusion bioreactor system', *Acta Biomater*, vol. 95, p. 236, Sep. 2019, doi: 10.1016/J.ACTBIO.2018.11.024.

[35] Y. Wen *et al.*, 'Factors influencing the measurement of the secretion rate of extracellular vesicles', *Analyst*, vol. 145, no. 17, pp. 5870–5877, Aug. 2020, doi: 10.1039/D0AN01199A.

[36] 'Low particle media, RoosterCollect-EV, and RoosterCollect-EV-CC support a seamless transition from hMSC expansion to EV collection'.

[37] 'Cell Number Total EV Production Cell Expan-sion Phase EV Collection Phase EXTRACELLULAR VESICLE (EV) PRODUCTION HIGH VOLUME hMSCs | BIOPROCESS MEDIA COLLECTION MEDIA & REAGENTS A Standardized System Drives Massive Yields. Tunable at Multiple Scales. REVOLUTIONIZING EXTRACELLULAR VESICLE PRODUCTION Transition from hMSC expansion to dependable EV collection During collection, EV Boost crosses you over to the Boost Zone TM', Accessed: Oct. 22, 2022. [Online]. Available: www.roosterbio.com.

[38] S. A. A. Kooijmans, R. M. Schiffelers, N. Zarovni, and R. Vago, 'Modulation of tissue tropism and biological activity of exosomes and other extracellular vesicles: New nanotools for cancer treatment', *Pharmacol Res*, vol. 111, pp. 487–500, Sep. 2016, doi: 10.1016/J.PHRS.2016.07.006.

[39] F. Royo, C. Théry, J. M. Falcón-Pérez, R. Nieuwland, and K. W. Witwer, 'Methods for Separation and Characterization of Extracellular Vesicles: Results of a Worldwide Survey Performed by the ISEV Rigor and Standardization Subcommittee', *Cells*, vol. 9, no. 9, Aug. 2020, doi: 10.3390/CELLS9091955.

[40] T. Liangsupree, E. Multia, and M. L. Riekkola, 'Modern isolation and separation techniques for extracellular vesicles', *J Chromatogr A*, vol. 1636, p. 461773, Jan. 2021, doi: 10.1016/J.CHROMA.2020.461773.

[41] S. Bosch *et al.*, 'Trehalose prevents aggregation of exosomes and cryodamage', *Scientific Reports 2016 6:1*, vol. 6, no. 1, pp. 1–11, Nov. 2016, doi: 10.1038/srep36162.

[42] S. I. van de Wakker *et al.*, 'Influence of short term storage conditions, concentration methods and excipients on extracellular vesicle recovery and function', *European Journal of Pharmaceutics and Biopharmaceutics*, vol. 170, pp. 59–69, Jan. 2022, doi: 10.1016/j.ejpb.2021.11.012.